



Chitosan hydrogel incorporated with dental pulp stem cell-derived exosomes alleviates periodontitis in mice via a macrophage-dependent mechanism

Zongshan Shen^{a,1}, Shuhong Kuang^{a,1}, Yong Zhang^{a,1}, Mingmei Yang^a, Wei Qin^a, Xuetao Shi^{b,**}, Zhengmei Lin^{a,*}

^a Hospital of Stomatology, Guangdong Provincial Key Laboratory of Stomatology, Guanghua School of Stomatology, Sun Yat-sen University, Guangzhou, Guangdong, China

^b National Engineering Research Centre for Tissue Restoration and Reconstruction, South China University of Technology, Guangzhou, China



ARTICLE INFO

Keywords:

Dental pulp stem cells
Exosomes
Chitosan hydrogel
Periodontitis
Macrophages

ABSTRACT

Periodontitis is caused by host immune-inflammatory response to bacterial insult. A high proportion of pro-inflammatory macrophages to anti-inflammatory macrophages leads to the pathogenesis of periodontitis. As stem cell-derived exosomes can modulate macrophage phenotype, dental pulp stem cell-derived exosomes (DPSC-Exo) can effectively treat periodontitis. In this study, we demonstrated that DPSC-Exo-incorporated chitosan hydrogel (DPSC-Exo/CS) can accelerate the healing of alveolar bone and the periodontal epithelium in mice with periodontitis. Gene Ontology (GO) term enrichment analysis showed that treatment with DPSC-Exo/CS ameliorated periodontal lesion by suppressing periodontal inflammation and modulating the immune response. Specifically, DPSC-Exo/CS facilitated macrophages to convert from a pro-inflammatory phenotype to an anti-inflammatory phenotype in the periodontium of mice with periodontitis, the mechanism of which could be associated with miR-1246 in DPSC-Exo. These results not only shed light on the therapeutic mechanism of DPSC-Exo/CS but also provide the basis for developing an effective therapeutic approach for periodontitis.

1. Introduction

Periodontitis is a destructive inflammatory disease of the periodontium, affecting the gingiva, periodontal ligament and alveolar bone [1,2]. Over 30% of adults worldwide have periodontitis. If left untreated, it leads to the loss of tooth support and even tooth loss [2]. Moreover, patients with periodontitis have an increased risk of diabetes [3], atherosclerosis [4] and Alzheimer's disease [5]. Current treatments for periodontitis focus on the removal of periodontal bacteria via mechanical debridement techniques, including scaling and root planing. Antibiotics are used as an adjunct therapy to mechanical debridement in patients with deep periodontal pockets [6]. However, due to the high recurrence of periodontitis, patients must receive these treatments repetitively [7]. Additionally, current treatments are not effective in over 30% patients with severe periodontitis [8,9].

Bacterial infection is an initial factor in the progression of periodontitis, but what ultimately induces periodontium destruction is dysregulation of the host immune-inflammatory response [10]. Specifically, pro-inflammatory cytokines, such as IL-1 and TNF- α , are responsible for periodontal inflammation and alveolar bone resorption [11,12]. Inhibition of TNF- α and IL-1 by blockade has been reported to alleviate periodontium inflammation and bone resorption in mouse models of periodontitis [11,12]. In addition, Treg-recruiting treatments have been proved to be effective in reducing alveolar bone loss in dog models of periodontitis by decreasing inflammatory cytokines, including TNF- α , IL-1 β and IL-17 [13]. Hence, modulating the host immune response could be an alternative treatment approach for periodontitis.

Macrophages activated by bacteria can release many inflammatory cytokines, causing gingiva destruction and alveolar bone resorption

Peer review under responsibility of KeAi Communications Co., Ltd.

* Corresponding author. Department of Operative Dentistry and Endodontics, Guanghua School of Stomatology, Guangdong Provincial Key Laboratory of Stomatology, Sun Yat-sen University, Guangzhou, 510030, China.

** Corresponding author. National Engineering Research Centre for Tissue Restoration and Reconstruction, South China University of Technology, Guangzhou, 510006, China.

E-mail addresses: shxt@scut.edu.cn (X. Shi), linzhm@mail.sysu.edu.cn (Z. Lin).

¹ These three authors contributed equally to this work.

<https://doi.org/10.1016/j.bioactmat.2020.07.002>

Received 22 April 2020; Received in revised form 1 July 2020; Accepted 2 July 2020

2452-199X/© 2020 The Authors. Publishing services by Elsevier B.V. on behalf of KeAi Communications Co., Ltd. This is an open access article under the CC BY-NC-ND license (<http://creativecommons.org/licenses/by-nc-nd/4.0/>).

[14–16]. Macrophages are divided into pro-inflammatory macrophages and anti-inflammatory macrophages [17]. Pro-inflammatory macrophages are important producers of many inflammatory cytokines, such as IL-1 β and TNF- α , and they can stimulate the activation of T cells and polymorphonuclear neutrophils, which cause alveolar bone loss [18]. In addition, pro-inflammatory macrophages can elevate local expression of RANKL, which promotes osteoclast differentiation in the periodontium [19]. By contrast, anti-inflammatory macrophages are involved in inflammation resolution and tissue regeneration via the secretion of anti-inflammatory mediators [20]. In the resolution of inflammation, anti-inflammatory macrophages contribute to efferocytosis of the apoptotic osteoblastic cells, mediating bone formation [21]. As the imbalance of pro-inflammatory/anti-inflammatory macrophages is responsible for periodontium destruction [22,23], converting the macrophage phenotype from pro-inflammatory to anti-inflammatory could effectively treat periodontitis.

As dental pulp stem cells (DPSCs) exhibit beneficial immunomodulatory and anti-inflammatory characteristics, they have been applied in treating many inflammatory diseases [24]. DPSCs are a population of dental-derived mesenchymal stem cells, with easy accessibility and minimal ethical concerns about their use [25]. DPSCs exhibit their immunomodulatory effects on macrophage phenotype in inflammatory diseases [26,27]. Current studies have indicated that the therapeutic effects of stem cells are mainly attributable to their release of paracrine factors [24,28]. As one of the most important paracrine mediators, stem cell-derived exosomes show therapeutic effects via immunomodulation [29,30].

Chitosan has been widely explored for tissue engineering and pharmaceutical application owing to its biocompatibility, biodegradability, and muco-adhesiveness [31]. Chitosan and β -sodium glycerophosphate (β -GP) can form a hydrogel at body temperature [32]. Mechanical properties of chitosan hydrogel (CS) can be tailored by varying the concentration of chitosan [31]. CS can repair tissue defects with irregular shapes by a simple injection of the pre-gel solution [33]. As a reliable drug-controlled release material, CS can release active drugs such as doxycycline, aspirin and antibiotics at the disease site [33,34]. Due to these advantages, CS has been widely explored for dental medicine [33]. For example, CS loaded with aspirin and erythropoietin promotes periodontium regeneration in rat models of periodontitis by suppressing periodontal inflammation [34]. CS has also been applied as an ideal injectable carrier to load cells and exosomes for the treatment of multiple diseases, such as hindlimb ischaemia [31,32]. Therefore, we investigated whether DPSC-Exo-incorporated CS (DPSC-Exo/CS) is effective in modulating macrophage phenotype and treating periodontitis.

Overall, this study aims to determine (i) whether DPSC-Exo/CS can reduce epithelial lesion and accelerate alveolar bone healing in mice with periodontitis, (ii) whether DPSC-Exo/CS can reduce periodontal inflammation by facilitating macrophages to convert from a pro-inflammatory phenotype to an anti-inflammatory phenotype in the periodontium of mice with periodontitis, and (iii) whether the DPSC-Exo/CS-mediated protective effect on the epithelium and alveolar bone in mice with periodontitis occurs partially via miR-1246.

2. Methods

2.1. Cells

DPSCs were obtained from exfoliated teeth of healthy donors, who provided informed consent. The use of the teeth for scientific purposes was approved and in accordance with the ethical guidelines set by the Ethics Committee of Guanghua School of Stomatology, Sun Yat-sen University (KQEC-2018-06). DPSCs were isolated from dental pulp tissues and cultured as previously described [35]. Briefly, pulp tissues were gently separated from the pulp chamber and cut into small fragments. Collagenase type I solutions (4 mg/ml; Sigma-Aldrich, MO, USA)

and dispase solutions (4 mg/ml; Sigma-Aldrich, MO, USA) were used to dissociate pulp tissue into single-cell suspensions, which were then seeded into a 25 cm² culture flask. DPSC growth medium consisted of Dulbecco's modified Eagle's medium with nutrient mixture F-12 (DMEM/F-12; Gibco; Thermo Fisher Scientific, MA, USA), 10% foetal bovine serum (FBS; Gibco; Thermo Fisher Scientific, USA) and 100 IU/ml penicillin/streptomycin (Sigma-Aldrich, MO, USA). We cultured DPSCs in a humidified 5% CO₂ water-jacketed incubator (Thermo Fisher Scientific, USA). The culture medium was changed every 3 days.

The mice were euthanized using isoflurane followed by cervical dislocation to ensure no discomfort to the mice. The mice were then sprayed with 70% ethanol and placed on a dissecting board. A small incision was made, and the skin was peeled back towards the limbs in order to expose the femurs. The muscle was then removed from the femurs. Bone marrow cells were collected from mouse femurs and differentiated for 7 days in RPMI 1640 medium (Gibco; Thermo Fisher Scientific, MA, USA) supplemented with 10% FBS, 2 mM L-glutamine, 1% penicillin/streptomycin and 20% L929 conditioned medium. On day 7, differentiated bone marrow-derived macrophages (BMDMs) were induced with medium containing lipopolysaccharide (LPS; 100 ng/ml; Sigma-Aldrich, MO, USA) and IFN- γ (10 ng/ml; Peprotech, Rocky Hill, NJ, USA) and incubated with CS, DPSC-Exo/CS (10 μ g exosome for 10⁵ cells), miRNA mimics (RiboBio, Guangzhou, China) or miRNA inhibitor (RiboBio, Guangzhou, China) for 24 h. MiRNA mimics and miRNA inhibitor were transfected with Lipofectamine 2000 (Invitrogen, CA, USA).

2.2. Isolation and characterization of exosomes

For exosome collection, 80% confluent cells were cultured with complete medium supplemented with 10% exosome-depleted FBS for 3 days. For exosome depletion, FBS was centrifuged at 120,000 \times g for 18 h, a duration demonstrated to be sufficient to remove approximately 95% of the extracellular vesicles from FBS. Conditioned medium from cultures of DPSC cells was centrifuged at 300 \times g for 10 min to remove any cells or large cellular fragments. Supernatants were then collected and transferred to ultracentrifuge tubes (Beckman Coulter, Brea, CA, USA). Samples were centrifuged for 20 min at 16,500 \times g to remove microvesicles. Supernatants were carefully collected and centrifuged at 120,000 \times g for 2.5 h at 4 $^{\circ}$ C. The exosome pellet was reconstituted in PBS and stored at -80° C.

The exosome concentration was measured with a bicinchoninic acid (BCA) Protein Assay Kit (CWBioTech, Beijing, China). Western blotting and flow cytometry were conducted to examine the exosome markers. The morphology of the exosomes was assessed with transmission electron microscopy (TEM; JEOL, Tokyo, Japan). In brief, exosomes were loaded onto a copper grid. After staining with 2% (w/v) phosphotungstic acid for 5 min, the exosomes were examined by TEM. The particle size distribution was identified by nanoparticle tracking analysis (NTA) with a NanoSight NS300 instrument (Malvern, Worcestershire, U.K.).

2.3. Labelling and internalization of exosomes

DPSC-Exo were labelled with fluorescent 3,3'-diiodoacetylcarbocyanine perchlorate (DiD; Invitrogen, CA, USA) according to the manufacturer's recommendations. Briefly, purified DPSC-Exo were incubated in 5 μ M DiD for 15 min at 37 $^{\circ}$ C and were then ultracentrifuged at 120,000 \times g for 90 min to remove unbound dye. After being washed twice in PBS with centrifugation at 120,000 \times g, the labelled exosomes were resuspended in PBS prior to use. BMDMs seeded on glass slides placed in 24-well plates were incubated at 37 $^{\circ}$ C with DiD-labelled DPSC-Exo-incorporated CS (1 μ g for 10⁵ cells). Uptake was stopped after 3 h by washing. Then, the cells were fixed in 4% paraformaldehyde (PFA) for 15 min and permeabilized in 0.1% Triton-X in PBS for 15 min. Samples were stained sequentially with Actin-Tracker Green

(Beyotime Institute of Biotechnology, Haimen, China) for 30 min and 4',6-diamidino-2-phenylindole (DAPI; Invitrogen, CA, USA) for 3 min at room temperature.

2.4. Preparation of CS hydrogel loaded with DPSC-Exo

The CS hydrogel preparation was based on previous studies [32]. Briefly, to obtain a 2% CS hydrogel, 50% β -glycerophosphate (Macklin, Shanghai, China) solution was added to a 2% CS (Macklin, Shanghai, China) solution at a 5:1 vol ratio on ice with constant stirring until the two solutions were completely mixed. For the preparation of CS hydrogel loaded with DPSC-Exo, the DPSC-Exo solution was mixed with 2% CS hydrogel at a 1:1 vol ratio. Then, the mixture was incubated at 37 °C for 30 min to cross-link into the hydrogel. The final concentration of CS was 1%.

The release profile of DPSC-Exo/CS was detected according to previous studies [32,36]. Briefly, 100 μ l of DPSC-Exo/CS was placed in a transwell chamber inserted in a 24-well plate and incubated with 500 μ l of PBS at 37 °C. A volume of 10 μ l of the supernatants was collected and replaced by the same volume of fresh PBS on the indicated days. The concentration of released exosomes was tested with the BCA Protein Assay Kit.

2.5. Animals

Six- to eight-week-old male C57BL/6J mice were purchased from the National Resource Center of Model Mice (Nanjing, China). All experiments were approved by the Animal Care and Use Committee of Sun Yat-sen University (SYSU-IACUC-2018-000096).

We established the periodontitis mouse model according to previous studies [34,37,38]. Briefly, a mouse was placed in a sealed container with a 4% (vol/vol) isoflurane flow until fully anaesthetized. A 5-0 silk ligature was tied around the maxillary left second molar of the isoflurane-anaesthetized mouse. The ligature was remained for 10 days to induce periodontitis. For exosome treatment, DPSC-Exo (50 μ g), DPSC-Exo/CS or an equal volume of PBS/CS was injected locally after ligature removal (Fig. 2A). For antagomir treatment, the mixture of DPSC-Exo/CS and antagomir was injected locally after ligature removal.

For micro-CT analysis, maxillae from experimental mice were collected, fixed in 4% PFA for 24 h, washed in PBS 3 times, dehydrated in 75% ethanol, placed in standardized cylindrical sample containers and scanned with high-resolution micro-CT (Scano Medical AG, Bassersdorf, Switzerland). Key parameters were set at 70 kV, 114 mA, 20 μ m increments, and a 3000-ms integration time. Three-dimensional microstructural image data were reconstructed and analysed using image analysis software (VGStudio MAX 1.2.1, Heidelberg, Germany). The distance between the cemento-enamel junction and the alveolar bone crest (CEJ-ABC distance) was measured at six predetermined sites on both the buccal and palatal sides, as previously described [38].

2.6. Histology and immunofluorescence (IF) staining

For histological analyses, the maxillae collected from experimental mice were fixed in 4% PFA and decalcified in 0.5 M EDTA for 3 weeks. Then, the maxillae were embedded in Tissue-Tek optimum cutting temperature (OCT) compound (Sakura Finetek, Torrance, CA, USA) and cut in a freezing microtome (Leica CM1900, Germany). Sections were stained with haematoxylin and eosin (H&E) and tartrate-resistant acid phosphatase (TRAP; Jiancheng Technology, Nanjing, China). TRAP-positive multinucleated (> 3 nuclei) cells were considered osteoclasts [38]. The CEJ-ABC distance was measured to evaluate bone loss.

For IF staining, the maxillae from experimental mice were embedded in Tissue-Tek OCT and cut in a freezing microtome (Leica CM1900, Germany). Sections (5 μ m thick) were placed on glass slides (CITOGLAS, Jiangsu, China), blocked with buffer containing 0.05% PBS-Tween and 0.5% FBS for 30 min, and sequentially incubated with

the appropriate primary antibodies overnight at 4 °C and secondary antibodies for 60 min at room temperature. Then, sections were counterstained with DAPI for 3 min at room temperature. IF signals were visualized and recorded using a LSM780 laser scanning confocal microscope (Zeiss, Germany).

2.7. Tissue extraction and single-cell preparations

The periodontium was collected after mice were sacrificed. Tissues were further processed to generate single-cell suspensions [39]. In brief, gingival tissues from experimental mice were cut into small fragments. Then, the fragments were added to RPMI 1640 medium containing 3 mg/ml collagenase type I and 4 mg/ml dispase and incubated at 37 °C for 60 min. The tissue fragments were filtered through a 70 μ m cell strainer (Biologix Research Company, USA) to remove tissue fragments and were then resuspended in fresh RPMI medium.

2.8. Flow cytometry

Single-cell suspensions were resuspended at a density of 10^6 cells/100 μ l in Zombie viability dye (BioLegend, San Diego, CA, USA) and incubated for 15 min at room temperature to exclude dead cells from the analysis. For surface antigen staining, the suspensions were sequentially incubated with Fc blocker (BioLegend, San Diego, CA, USA) at 4 °C for 10 min and with the appropriate antibody in the dark at 4 °C for 30 min. For intracellular antigen staining, after cell surface antigens were stained, cells were fixed in fixation buffer (0.5 ml/tube; BioLegend, San Diego, CA, USA) in the dark for 20 min and centrifuged at $350 \times g$ for 5 min according to the manufacturer's recommendations. A predetermined antibody of interest was added, and the samples were incubated in the dark at 4 °C for 20–30 min. The cells were washed, resuspended and analysed by flow cytometry (FACScan; Becton Dickinson, San Diego, CA, USA). Gating strategies for the flow cytometric analysis of cultured cells and periodontal cells are shown in Figs. S1–2. Each analysis was performed with data from at least three independent experiments. The data were analysed with FlowJo V10.0 (Treestar, Ashland, OR, USA).

2.9. RNA extraction, reverse transcription, and RT-qPCR

Total RNA was extracted from periodontal tissue and cells with TRIzol reagent (Invitrogen, Carlsbad, CA, USA), and cDNA was generated with PrimeScript RT Master Mix (Toyobo Co, Ltd, Osaka, Japan). The expression level of genes was measured by qPCR in a Bio-Rad CFX96™ Detection System (Roche, Sweden) with SYBR PCR Master Mix (Roche, Indianapolis, IN, USA). Small RNA was extracted from cells with an miRNA isolation kit (Qiagen, Hilden, Germany), and cDNA was generated with an miRNA reverse transcription kit (Shengggong, Shanghai, China). The expression level of miRNAs was measured by qPCR in a Bio-Rad CFX96™ Detection System with SYBR PCR Master Mix. U6 was used as the internal reference. The primers used are shown in Supplementary Table S1.

2.10. RNA sequencing analysis

The periodontium was extracted from mice treated with DPSC-Exo/CS or CS. RNA was isolated from the periodontium with TRIzol reagent. RNA sequencing libraries were constructed using an NEBNext® Ultra™ RNA Library Prep Kit and were then subjected to deep sequencing with Illumina Sequencing (HiSeq, Fasteris SA, Switzerland) at GENEWIZ Co. Ltd., Suzhou, China. Small RNAs of DPSC-Exo were extracted and used for miRNA sequencing. miRNA libraries were constructed and were then subjected to deep sequencing with the Illumina HiSeq 2500 platform at RiboBio Co. Ltd., Guangzhou, China.

Bioconductor was used to analyse the raw gene count matrix. The FastQC tool was used for quality control of raw sequencing data.

Differentially expressed genes (DEGs) were analysed by using the edgeR analysis package in the R statistical programme with the criteria of an adjusted p value ≤ 0.05 and an absolute \log_2 (fold change) > 2 . RStudio was used to create heatmaps and volcano plots. Gene Ontology (GO) term enrichment analysis was performed for the top 200 down-regulated DEGs using the Database for Annotation, Visualization and Integrated Discovery (DAVID). The DAVID enrichment table is shown in [Supplementary Table S2](#).

2.11. Western blot analysis

Protein was extracted from cells and tissues in each group with radioimmunoprecipitation assay (RIPA) buffer (Millipore, MA, USA) on ice. RIPA buffer-extracted lysates were further disrupted with an ultrasonic homogenizer and centrifuged at $12,000 \times g$. The total protein concentration in the lysates was measured using a BCA protein assay kit (CWBioTech, Beijing, China). Sodium dodecyl sulfate-polyacrylamide gel electrophoresis (SDS-PAGE) was performed to separate the proteins, which were then transferred to a polyvinylidene fluoride (PVDF) membrane (Millipore, MA, USA). A buffer containing 5% bovine serum albumin was applied to block the membranes for 30 min at room temperature. PVDF membranes containing proteins were sequentially incubated with the indicated primary antibodies at 4 °C overnight and with horseradish peroxidase-conjugated secondary antibodies for 1 h at room temperature. A chemiluminescence kit (Millipore, MA, USA) was applied to detect the target bands. The antibody information is listed in [Supplementary Table S3](#).

2.12. Cytokine measurements

Cytokines in protein lysates were measured using the LEGENDplex™ Mouse Inflammation Panel (BioLegend, San Diego, CA, USA). The total protein concentration of samples from experimental mice was measured using a BCA protein assay kit, and equal amounts of total protein were used for the following assay. In brief, the capture beads were conjugated to specific antibodies, rendering them easily differentiated by size and internal fluorescence. The capture beads were incubated with the biological samples containing target analytes specific for the capture antibodies at room temperature for 2 h. Next, a biotinylated detection antibody was added and detected by flow cytometry. LEGENDplex8.0 data analysis software was used to calculate the mean fluorescence intensity (MFI) of each cytokine. Cytokine concentrations were determined by comparing the fluorescence intensity to a standard.

2.13. Statistical analysis

All data are presented as the means \pm SEMs of at least three independent experiments. Comparisons between groups were performed using one-way ANOVA with Tukey's post hoc test. $P < 0.05$ was considered statistically significant. All statistical analyses were performed with Prism software (GraphPad).

3. Results

3.1. Characterization of DPSC-Exo and DPSC-Exo/CS

DPSC-Exo were isolated from conditioned medium of DPSCs by serial ultracentrifugation (UC) and were then identified by various methods, including western blotting, TEM, flow cytometry and NTA. Western blot analysis showed that DPSC-Exo expressed CD9, heat shock protein 70 (HSP70) and tumour susceptibility 101 protein (TSG101), which are commonly enriched in exosomes. In addition, the cytosolic marker β -tubulin was absent in DPSC-Exo ([Fig. 1A](#)). TEM analysis revealed that DPSC-Exo were spherically shaped vesicles with a bilayer membrane structure ([Fig. 1B](#)). NTA showed that the diameters of DPSC-Exo (d.nm) ranged from 50 to 200 nm ([Fig. 1C](#)). Moreover, flow

cytometric analysis showed that DPSC-Exo exhibited high expression levels of exosome markers, including CD63 and CD81 ([Fig. 1D](#)). Collectively, these results demonstrated that we successfully isolated DPSC-Exo.

As CS could enhance the stability of exosomes, it has been applied as an ideal injectable carrier to load exosomes for the treatment of multiple diseases [31,32]. We combined DPSC-Exo with CS to generate DPSC-Exo/CS. The DPSC-Exo/CS mixture was in a translucent liquid state at 4 °C but transitioned to hydrogel at 37 °C ([Fig. 1E](#)). To measure the release ratio of exosomes from DPSC-Exo/CS, we submerged DPSC-Exo/CS in PBS at 37 °C. Then, BCA assays were performed to determine the concentration of exosomes in PBS from day 0 to day 10. Most of the loaded exosomes were released within 7 days. In addition, the loading efficiency of exosomes in DPSC-Exo/CS was approximately 80% ([Fig. 1F](#)). These results demonstrated that we successfully prepared DPSC-Exo/CS.

3.2. DPSC-Exo/CS rescues epithelial lesion and alveolar bone loss in P mice

We investigated the therapeutic effects of DPSC-Exo/CS in mice with experimental periodontitis (P mice). Periodontal tissues were collected from the experimental mice for micro-CT and histological analyses ([Fig. 2A](#)). As periodontitis presents with alveolar bone resorption [2], we investigated the impact of DPSC-Exo/CS on the alveolar bone. Micro-CT analysis showed that alveolar bone loss was lower in the DPSC-Exo/CS-treated group than in the PBS-, CS- or DPSC-Exo-treated groups ([Fig. 2B, E](#)). In addition, H&E staining analysis revealed that the epithelial layers of periodontal tissues were thickest, the number of infiltrating inflammatory cells was lowest, and the amount of alveolar bone was greater in the DPSC-Exo/CS-treated group than in the PBS-, CS- and DPSC-Exo-treated groups after 10 days ([Fig. 2C, F](#)). Osteoclast cells participate in bone resorption and negatively regulate the formation of neonatal alveolar bone [38]. TRAP staining analysis revealed fewer osteoclasts in the periodontal tissues of the DPSC-Exo/CS-treated group than in those of the PBS-, CS- and DPSC-Exo-treated groups ([Fig. 2D, G](#)). These results indicate that DPSC-Exo/CS infusion alleviates experimental periodontitis and rescues alveolar bone loss in P mice.

3.3. DPSC-Exo/CS alleviates periodontal inflammatory response in P mice

The persistent inflammatory response is responsible for the aberrant repair of periodontitis-induced damage. We further confirmed the effects of DPSC-Exo/CS on alleviating periodontal inflammation in P mice. LEGENDplex™ bead-based immunoassays demonstrated that the levels of IL-23, IL-1 α , TNF- α , IL-12, IL-1 β , IL-27, and IL-17 were significantly reduced in periodontal tissues extracted from DPSC-Exo/CS-treated mice compared with those in PBS-, CS- or DPSC-Exo-treated mice ([Fig. 3A](#)).

As upregulation of the nuclear factor κ B (NF- κ B) p65 and p38 mitogen-activated protein kinase (MAPK) signalling pathways causes the persistence of periodontal inflammation [40], we examined whether DPSC-Exo/CS downregulated the NF- κ B p65 and p38 MAPK signalling pathways in P mice. Western blot analysis confirmed the downregulation of NF- κ B p65 and p38 MAPK signalling in the DPSC-Exo/CS-treated group compared with those in the PBS-, CS- and DPSC-Exo-treated groups ([Fig. 3B, C, D, E](#)). Taken together, these results show that DPSC-Exo/CS can reduce periodontal inflammation in P mice.

3.4. DPSC-Exo/CS downregulate the chemotaxis pathway, inflammatory response and immune response in P mice

To investigate the mechanisms responsible for the therapeutic effects of DPSC-Exo/CS in P mice, we performed RNA sequencing analysis of the periodontium from DPSC-Exo/CS-treated P mice and CS-treated P mice. Approximately 7351 genes were deregulated (adjusted p

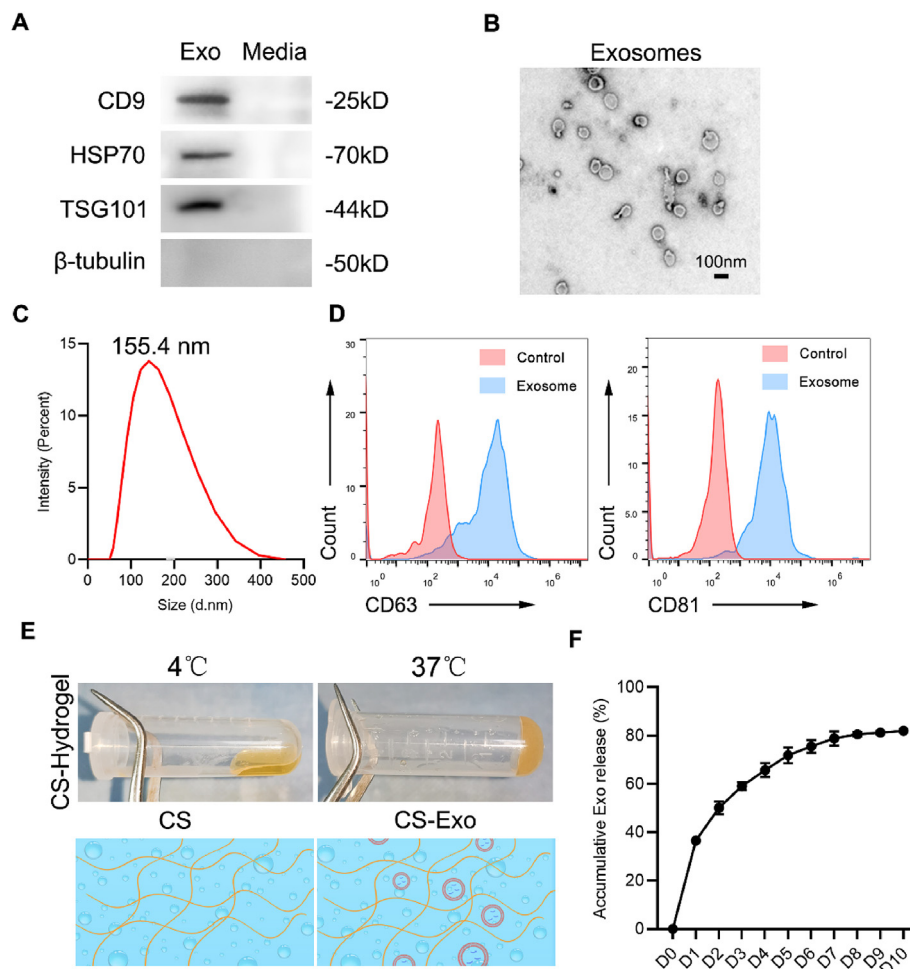


Fig. 1. Characterization of DPSC-Exo and DPSC-Exo/CS. (A) Representative western blots showing exosome markers (CD9, HSP70, and TSG101) and a cytosolic marker (β -tubulin) of DPSC-Exo and DPSC conditioned media. (B) TEM images of DPSC-Exo morphology. Scale bar = 100 nm. (C) Representation of particle size analysed using NTA. (D) Flow cytometry analysis of CD63 and CD81 expression on DPSC-Exo. (E) Synthesis process and schematic illustration of CS hydrogel. (F) The release curves of DPSC-Exo from the CS hydrogel.

value ≤ 0.05 and absolute \log_2 (fold change) > 2) in the periodontium of DPSC-Exo/CS-treated P mice and CS-treated P mice (Fig. 4A, B, C). Pro-inflammatory genes, such as IL-1 β (13.57-fold), IL-6 (6.78-fold), and TNF (4.25-fold), were downregulated in DPSC-Exo/CS-treated P mice compared with those in CS-treated P mice. We next conducted GO term enrichment analysis of the top 200 DEGs based on the biological process category. GO term enrichment analysis showed that the DEGs were significantly enriched in terms including neutrophil chemotaxis, chemokine-mediated signalling pathway, inflammatory response and immune response (Fig. 4D). Heatmaps of DEGs in enriched GO pathways showed that DEGs associated with the chemotaxis pathway (Fig. 4E), inflammatory response (Fig. 4F) and immune response (Fig. 4G) were downregulated in DPSC-Exo/CS-treated P mice compared with those in the CS-treated P mice. Taken together, the GO term enrichment analysis results show that DPSC-Exo/CS downregulate both the inflammatory response and immune response in P mice.

3.5. DPSC-Exo/CS facilitates macrophages to convert from a pro-inflammatory phenotype to an anti-inflammatory phenotype in the periodontium of P mice

Because of their participation in the phagocytosis of tissue debris and the resolution of tissue inflammation, macrophages play an important role in tissue repair [15,16]. Their conversion from a pro-inflammatory to an anti-inflammatory phenotype is crucial for

inflammation resolution [16,17]. Hence, we examined the phenotype of macrophages in the periodontium of P mice after DPSC-Exo/CS treatment. CD206⁺ cells are considered anti-inflammatory macrophages [16] that promote the healing of periodontitis. IF analysis showed significantly more CD206⁺ cells in the periodontal tissues of DPSC-Exo/CS-treated P mice than in PBS-, CS- and DPSC-Exo-treated P mice (Fig. 5A and B). In addition, PCR analysis showed that the gene expression level of CD206 was increased in the periodontium of DPSC-Exo/CS-treated P mice compared with those in PBS-, CS- and DPSC-Exo-treated P mice (Fig. 5C). CD11b⁺F4/80⁺ cells in the periodontium are widely considered to be macrophages [16]. Flow cytometric analysis showed that the expression of the anti-inflammatory marker CD206 was significantly increased and that the expression of the pro-inflammatory marker CD86 was significantly decreased in macrophages from the periodontium of DPSC-Exo/CS-treated P mice compared with those in PBS-, CS- and DPSC-Exo-treated P mice (Fig. 5D, E, F, G; Fig. S1). Taken together, these findings reveal that DPSC-Exo/CS facilitates macrophages to convert from a pro-inflammatory phenotype to an anti-inflammatory phenotype in the periodontium of P mice.

3.6. DPSC-Exo/CS facilitates macrophages to convert from a pro-inflammatory phenotype to an anti-inflammatory phenotype *in vitro*

BMDMs have been widely used as an *in vitro* model to investigate the phenotype of macrophages [41]. To evaluate the impact of DPSC-

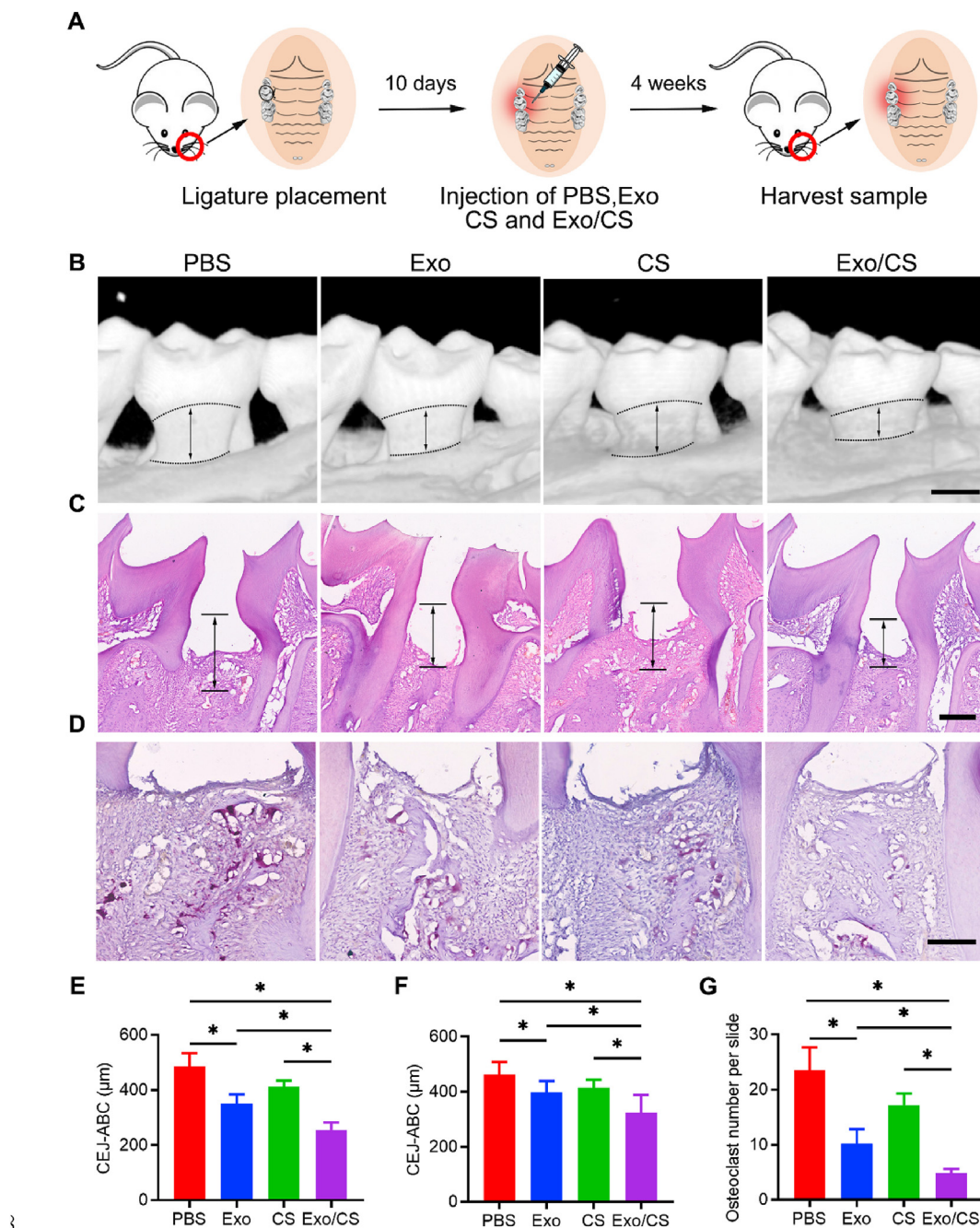


Fig. 2. DPSC-Exo/CS rescues epithelial lesion and alveolar bone loss in P mice. (A) A flow diagram showing the time of periodontal injection. (B) 3D reconstructions of maxillae of PBS-, CS-, DPSC-Exo- and DPSC-Exo/CS-treated groups ($n = 6$ per group) were generated by micro-CT. The vertical line extends from the CEJ to the ABC. The CEJ-ABC distance was measured at six predetermined sites on both the buccal and palatal sides. Scale bar = 400 μm . (C) Histological H&E-stained sections of the periodontium from each group are shown. The vertical line extends from the CEJ to the ABC. The CEJ-ABC distance was quantified in each microscope field of view. Scale bar = 200 μm . (D) Histological TRAP-stained sections of the periodontium from each group are shown. Osteoclasts are stained red. The number of osteoclasts was quantified in each microscope field of view. Scale bar = 100 μm . (E) Statistical analysis of the CEJ-ABC distance in each group ($n = 6$ per group) as determined by micro-CT. Error bar represents SEM. $*p < 0.05$. (F) Statistical analysis of the CEJ-ABC distance in each group ($n = 6$ per group) as determined by H&E staining. Error bar represents SEM. $*p < 0.05$. (G) Statistical analysis of the number of osteoclasts in each group ($n = 6$ per group) as determined by TRAP staining. Error bar represents SEM. $*p < 0.05$.

Exo/CS on BMDMs, we co-cultured BMDMs with DiD-labelled DPSC-Exo-incorporated CS by using a transwell system. IF analysis showed that BMDMs internalized exosomes within their cytoplasm (Fig. 6A). Flow cytometric analysis further confirmed that BMDMs could take up DiD-labelled DPSC-Exo (Fig. 6B).

Furthermore, BMDMs were cultured and stimulated with LPS and IFN- γ to mimic pro-inflammatory macrophages in the inflamed periodontium. Flow cytometric analysis showed that DPSC-Exo/CS-treated

BMDMs expressed significantly higher levels of the anti-inflammatory markers Arg and CD206 and lower levels of the pro-inflammatory markers iNOS and CD86 than untreated BMDMs (Fig. 6C and D; Fig. S2). PCR analysis showed that the expression levels of genes related to the anti-inflammatory phenotype of macrophages, such as CD206, Arg and CD163, were increased and that those related to the pro-inflammatory phenotype of macrophages, such as TNF α , IL-1 β , IL-6, iNOS and CD86, were decreased in DPSC-Exo/CS-treated BMDMs compared

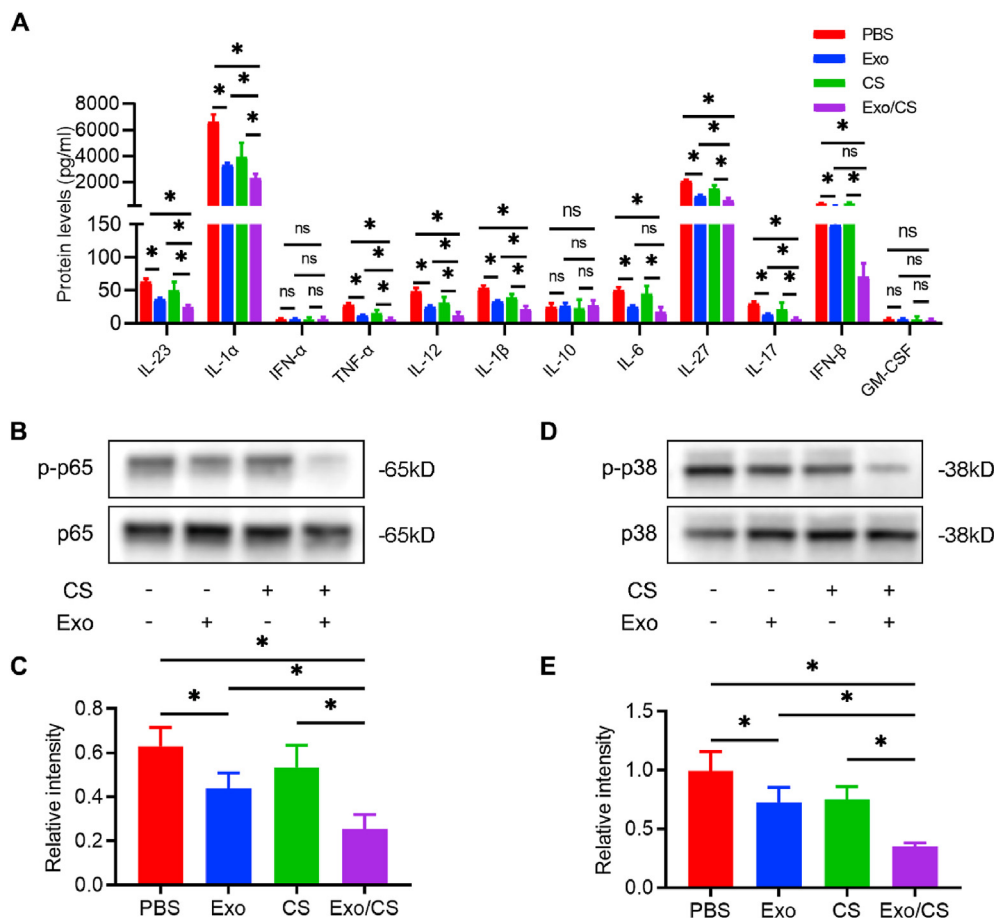


Fig. 3. DPSC-Exo/CS alleviates periodontal inflammatory response in P mice. (A) The levels of various inflammatory cytokines in the periodontium of PBS-, CS-, DPSC-Exo- and DPSC-Exo/CS-treated groups were analysed by LEGENDplex™ bead-based immunoassays (n = 6 per group). Error bar represents SEM. **p* < 0.05. (B) Representative western blots showing the NF-κB p65 signal pathway in the periodontium of each group (n = 6 per group). (C) Statistical analysis of western blots to determine the relative intensity of the NF-κB p65 signal pathway of each group (n = 6 per group). Error bar represents SEM. **p* < 0.05. (D) Representative western blots showing the p38 MAPK signal pathway in the periodontium of each group (n = 6 per group). (E) Statistical analysis of western blots to determine the relative intensity of the p38 MAPK signal pathway of each group (n = 6 per group). Error bar represents SEM. **p* < 0.05.

with untreated BMDMs (Fig. 6E). Taken together, these results indicate that DPSC-Exo/CS facilitates macrophages to convert from a pro-inflammatory phenotype to an anti-inflammatory phenotype.

3.7. miR-1246 in DPSC-Exo facilitates macrophages to convert from a pro-inflammatory phenotype to an anti-inflammatory phenotype *in vitro*

To explore the underlying mechanism by which DPSC-Exo facilitates conversion of macrophage inflammatory phenotype, miRNA-seq was performed to investigate the miRNA expression profiles of DPSC-Exo. The data showed that the most abundant miRNA, miR-1246, accounted for 43.9% of the total miRNA reads (Fig. 7A). PCR analysis confirmed that in DPSC-Exo, the expression level of miR-1246 was higher than in other miRNAs (Fig. 7B).

Furthermore, miR-1246 inhibitor and mimics were used to investigate the key role of miR-1246 in macrophage inflammatory phenotype conversion. Flow cytometric analysis showed that levels of the anti-inflammatory marker CD206 were decreased and levels of the pro-inflammatory marker CD86 were increased in BMDMs treated with DPSC-Exo + miR-1246 inhibitor compared with those treated with DPSC-Exo alone (Fig. 7C and D). Moreover, miR-1246 mimics facilitated macrophages to convert from a pro-inflammatory phenotype to an anti-inflammatory phenotype, which was in accordance with the effect of DPSC-Exo. Flow cytometric analysis showed that miR-1246 mimic-treated BMDMs expressed significantly higher levels of the anti-inflammatory marker CD206 and lower levels of the pro-inflammatory marker CD86 than untreated BMDMs (Fig. 7E and F). Taken together, these results indicate that miR-1246 in DPSC-Exo facilitates macrophages to convert from a pro-inflammatory phenotype to an anti-inflammatory phenotype.

3.8. Antagomir-1246 reverses the effects of DPSC-Exo/CS in mitigating epithelial lesion and alveolar bone loss in P mice

To investigate whether miR-1246 is important and involved in DPSC-Exo-mediated periodontal protection *in vivo*, we further used antagomir-1246 in the periodontitis mouse model. Micro-CT and histological analyses showed that antagomir-1246 remarkably reduced the effect of DPSC-Exo-mediated periodontal protection in P mice. Micro-CT analysis showed that alveolar bone loss was higher in the DPSC-Exo/CS + antagomir-1246-treated group than in the DPSC-Exo/CS-treated groups (Fig. 8A and B). In addition, H&E staining analysis revealed that the epithelial layers of periodontal tissues were thinner, the number of infiltrating inflammatory cells was higher, and the amount of neonatal alveolar bone was lower in the DPSC-Exo/CS + antagomir-1246-treated group than in the DPSC-Exo/CS-treated groups (Fig. 8C and D). TRAP staining analysis revealed more osteoclasts in the periodontal tissues of the DPSC-Exo/CS + antagomir-1246-treated group than in the DPSC-Exo/CS-treated group (Fig. 8E and F).

Moreover, IF analysis showed that the number of CD206⁺ anti-inflammatory macrophages was significantly reduced in the periodontal tissues of the DPSC-Exo/CS + antagomir-1246-treated group compared to that in the DPSC-Exo/CS-treated group (Fig. 8G and H). Western blot analysis further confirmed the upregulation of NF-κB p65 and p38 MAPK signalling in the DPSC-Exo/CS + antagomir-1246-treated group versus that in the DPSC-Exo/CS-treated group (Fig. 8I and J). These results indicate that antagomir-1246 abrogates the effects of DPSC-Exo in rescuing epithelial lesion and alveolar bone loss in P mice.

4. Discussion

In this study, we found that DPSC-Exo/CS alleviated periodontitis-

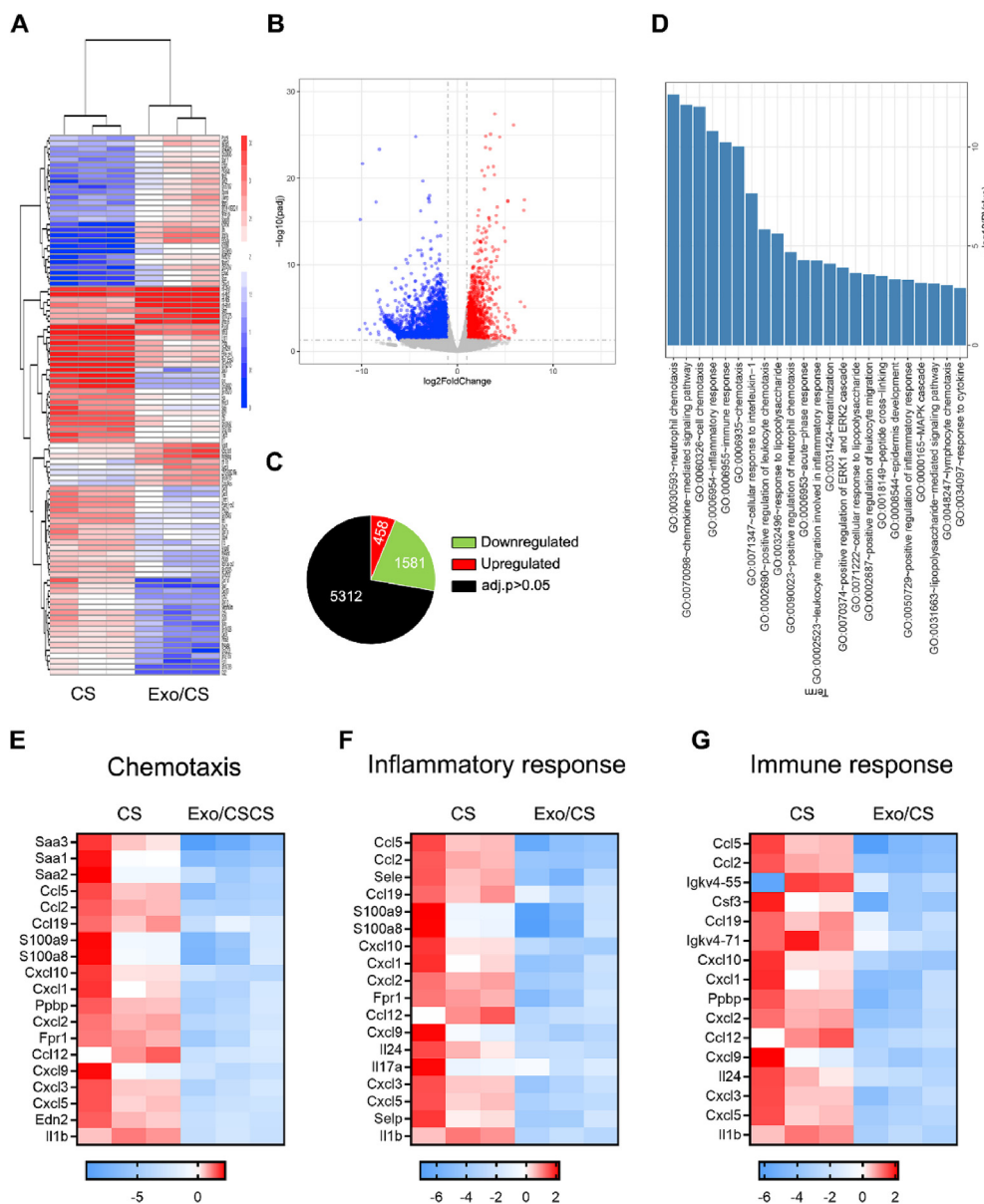


Fig. 4. DPSC-Exo/CS downregulate the chemotaxis pathway, inflammatory response and immune response in P mice. (A) Heatmap of DEGs in the periodontium of DPSC-Exo/CS-treated group versus the periodontium of CS-treated group (n = 3 per group). (B) Volcano plots showing DEGs. (C) Pie chart showing the number of dysregulated genes. (D) Gene Ontology (GO) functional analysis of the top 200 deregulated genes in the periodontium of the DPSC-Exo/CS-treated group compared with the CS-treated group. (E) Heatmaps of DEGs from the chemotaxis pathway in the periodontium of the DPSC-Exo/CS-treated group compared with the CS-treated group. (F) Heatmaps of DEGs from the inflammatory response pathway in the periodontium of the DPSC-Exo/CS-treated group compared with the CS-treated group. (G) Heatmaps of DEGs from the immune response pathway in the periodontium of the DPSC-Exo/CS-treated group compared with the CS-treated group.

induced epithelial lesion and reduced alveolar bone loss in experimental mice. Moreover, DPSC-Exo/CS suppressed periodontal inflammation by facilitating macrophages to convert from a pro-inflammatory phenotype to an anti-inflammatory phenotype in the periodontium of the mice with periodontitis.

Stem cell-derived exosomes exert therapeutic effects in various diseases via their anti-inflammatory and immunomodulatory capabilities [42]. Additionally, exosome infusion rarely induces immune reactions because exosomes do not contain MHC class I or II molecules [43]. However, the rapid clearance of unconjugated exosomes *in vivo* limits its therapeutic effects [44]. CS has been proved to be an ideal carrier to load exosomes, with characteristics of biodegradability, biocompatibility, swelling degree and mechanical resistance [32,34,45]. CS can also prolong the residence time of exosomes in the injured sites by protecting them from clearance by the immune system [32]. Our *in vitro* study showed that DPSC-Exo could be released sustainably from CS. Furthermore, DPSC-Exo/CS enhanced the therapeutic effects of DPSC-Exo by suppressing periodontium inflammation and reducing alveolar bone loss in P mice. Hence, CS is an ideal carrier for DPSC-Exo for treating periodontitis.

To further investigate the effects and mechanisms of DPSC-Exo in

periodontitis treatment, we performed RNA sequencing analysis of the periodontium from DPSC-Exo/CS-treated P mice and CS-treated P mice. GO term enrichment analysis showed that the efficiency of DPSC-Exo/CS in treating periodontitis was associated with their anti-inflammatory and immunomodulatory capabilities. To investigate the anti-inflammatory therapeutic effects of DPSC-Exo in periodontitis, we examined the inflammatory state of the periodontium in experimental mice. LEGENDplex™ bead-based immunoassays and PCR analysis showed that the levels of various inflammatory mediators were decreased in DPSC-Exo/CS-treated P mice compared with those of CS-treated P mice. Previous studies indicated that the activation of NF-κB and p38 MAPK signalling is responsible for persistent inflammation of the periodontium [40,46]. Our study showed that DPSC-Exo/CS infusion downregulated the activation of NF-κB and p38 MAPK signalling in the periodontium of P mice. All these results show that DPSC-Exo/CS can reduce periodontal inflammation in P mice.

Macrophages are the key regulators of periodontal inflammation and repair [16,47]. Although pro-inflammatory and anti-inflammatory macrophages play divergent roles in tissue injury and repair, their presence in a well-organized order is important for ideal tissue reconstruction [48,49]. The imbalance of pro-inflammatory/anti-

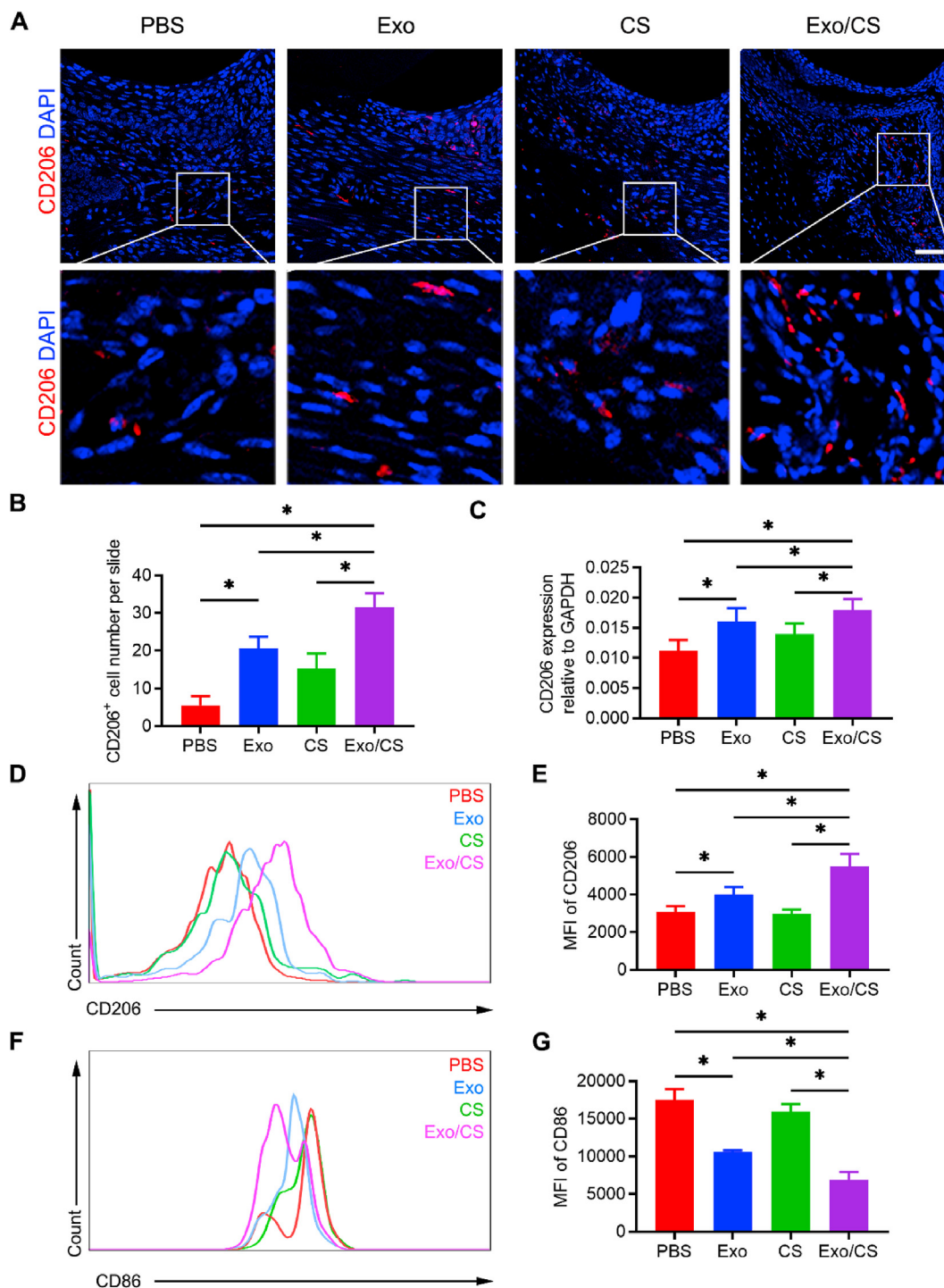


Fig. 5. DPSC-Exo/CS facilitates macrophages to convert from a pro-inflammatory phenotype to an anti-inflammatory phenotype in the periodontium of P mice. (A) Representative IF images of CD206⁺ cells in the periodontium of PBS-, CS-, DPSC-Exo- and DPSC-Exo/CS-treated groups (n = 6 per group). Nuclei were stained with DAPI. Scale bar = 100 μ m. (B) Statistical analysis of the IF staining of periodontal CD206⁺ cells in each group (n = 6 per group). The number of CD206⁺ cells was quantified for each microscope field of view. Error bars represent SEM. **p* < 0.05. (C) CD206 levels in gingiva extracted from the periodontium in each group were analysed by RT-qPCR (n = 6 per group). Error bars represent SEM. **p* < 0.05. (D) Representative density plots of CD206⁺ cells in the periodontium of the DPSC-Exo-treated group and PBS-treated group. Gates captured single, live CD11b⁺F4/80⁺ cells. (E) Statistical analysis of the flow cytometry data describing the MFI of CD206⁺ cells in the CD11b⁺F4/80⁺ cell population of the periodontium in each group (n = 6 per group). Error bars represent SEM. **p* < 0.05. (F) Representative density plots of CD86⁺ cells in the periodontium of the DPSC-Exo-treated group and PBS-treated group. Gates captured single, live CD11b⁺F4/80⁺ cells. (G) Statistical analysis of the flow cytometry data describing the MFI of CD86⁺ cells in the CD11b⁺F4/80⁺ cell population in the periodontium of each group (n = 6 per group). Error bars represent SEM. **p* < 0.05.

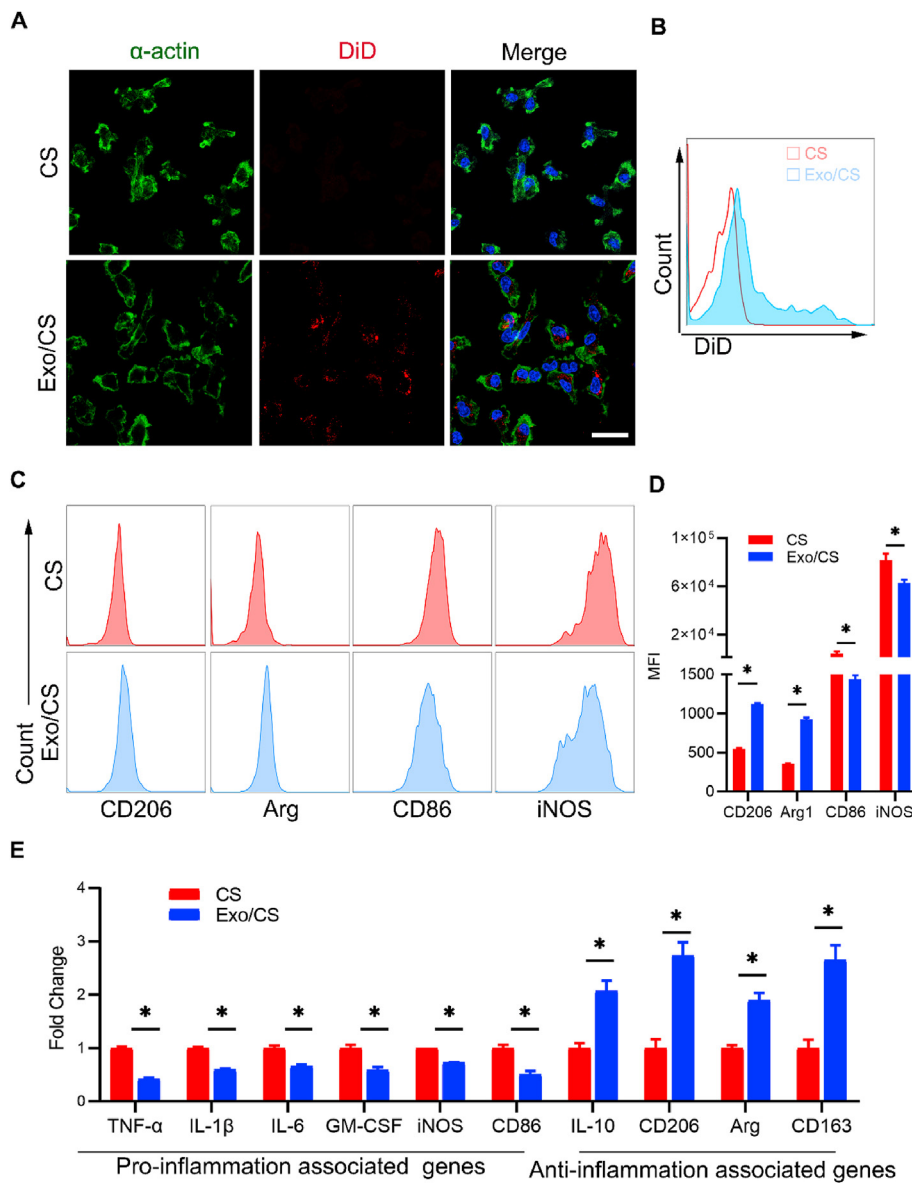


Fig. 6. DPSC-Exo/CS facilitates macrophages to convert from a pro-inflammatory phenotype to an anti-inflammatory phenotype *in vitro*. (A) Representative IF images of exosome internalization from BMDMs co-cultured with DPSC-Exo/CS and CS. Nuclei were stained with DAPI. Scale bar = 100 μ m. (B) Representative density plots of exosome internalization from BMDMs co-cultured with DPSC-Exo/CS (red line) and CS (blue line). (C) Representative density plots of phenotypic characterization of BMDMs co-cultured with DPSC-Exo/CS and CS (n = 6 per group). Gates captured single, live CD11b⁺F4/80⁺ cells. (D) Statistical analysis of the flow cytometry data describing the MFI of CD206, Arg, CD86, and iNOS cells with the FMO control in the CD11b⁺F4/80⁺ cell population of BMDMs co-cultured with DPSC-Exo/CS and CS (n = 6 per group). Error bar represents SEM. **p* < 0.05. (E) The mRNA expression levels of various cytokines and chemokines in BMDMs co-cultured with DPSC-Exo/CS and CS were analysed by RT-qPCR (n = 6 per group). **p* < 0.05.

inflammatory macrophages can cause persistent inflammation in the periodontium [22]. Persistent inflammation leads to aberrant repair of the periodontium. Specifically, proinflammatory cytokines such as TNF- α can induce NF- κ B activation in osteoblasts, which is a critical process in alveolar bone resorption [50]. The inflammatory microenvironment also contributes to the suppression of periodontal cell differentiation, thereby limiting regeneration of the periodontium [51]. The mechanism by which the exosomes of stem cells improve regeneration outcomes were considered to be their roles in improving the local microenvironment [52,53]. Therefore, we investigated whether DPSC-Exo/CS can improve the periodontal microenvironment by modulating macrophage phenotype. Interestingly, we found that DPSC-Exo facilitated macrophages to convert from a pro-inflammatory phenotype to an anti-inflammatory phenotype *in vitro*. Additionally, DPSC-Exo/CS increased the number of anti-inflammatory macrophages in the periodontium of P mice.

Recent studies have indicated that stem cell-derived exosomes contain miRNAs such as miR-223 [41] and miR-182 [54] that play roles in modulating the phenotype of macrophages. Therefore, one of the important mechanisms of the immunomodulatory effects of stem cell exosomes is exosome-mediated transfer of miRNAs. Our miRNA sequencing data showed that miR-1246 was the most highly expressed

among microRNAs in DPSC-Exo. Further, we demonstrated that miR-1246 mediated the effects of DPSC-Exo by facilitating macrophages to convert from a pro-inflammatory phenotype to an anti-inflammatory phenotype. Antagomir-miR-1246 dramatically attenuated the protective effect of DPSC-Exo/CS on alveolar bone and the periodontal epithelium in mice with periodontitis. These results showed the partial protective effects of DPSC-Exo/CS on epithelium and alveolar bone in mice with periodontitis via miR-1246.

Although we demonstrated that DPSC-Exo/CS can effectively treat periodontitis in mice, exosomes from other stem cell sources may be effective for treating periodontitis. Due to their accessibility, mesenchymal stem cells (MSCs) of dental origin are attractive sources of MSCs [25]. DPSCs and periodontal ligament stem cells (PDLSCs) are the most widely used MSCs of dental origin in treating periodontitis [55]. Therefore, exosomes derived from PDLSCs may be effective for treating periodontitis. An *in vitro* study shows that PDLSC-derived exosomes are a potential strategy to treat periodontitis by modulating the T helper cell 17/regulatory T cell balance [56]. Considering PDLSCs isolated from periodontal tissues from the root surface, these cells are easily affected by the local microenvironment of the donors [57]. Additionally, DPSCs are more easily obtained than PDLSCs. Thus, we investigated the effects of DPSC-Exo in treating periodontitis in mice. A

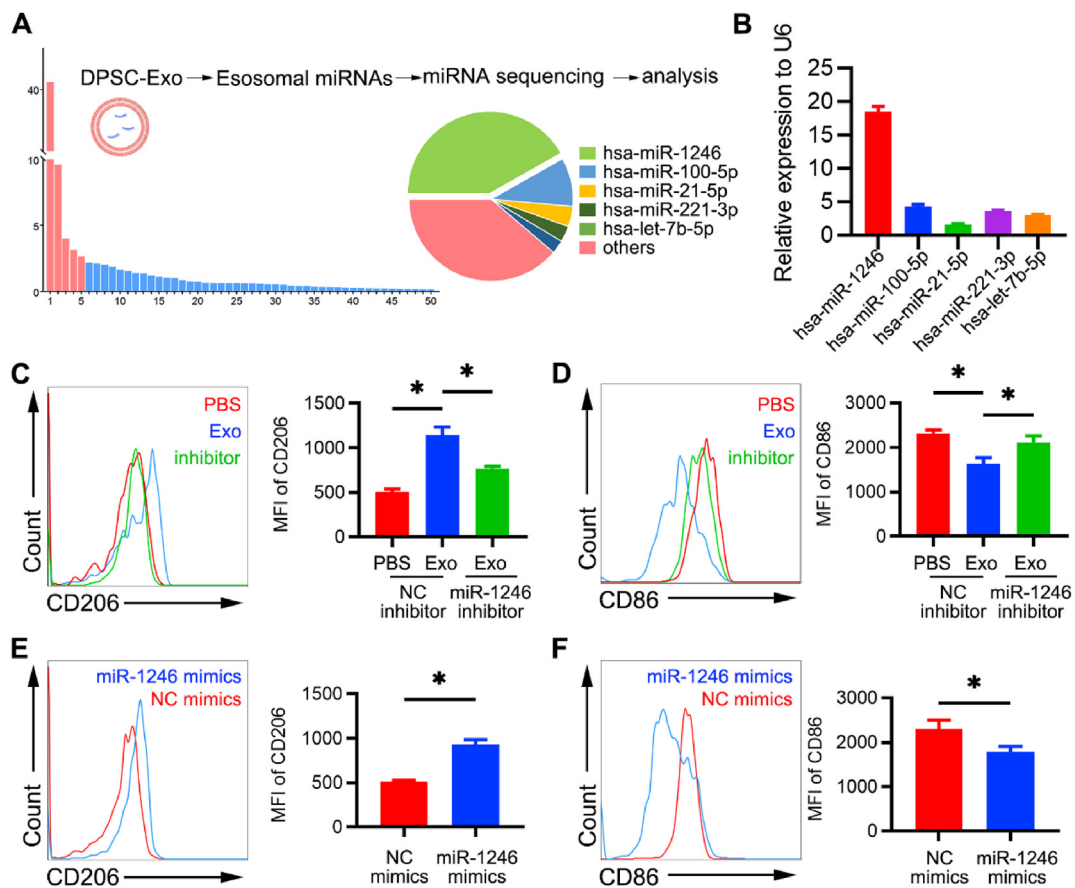


Fig. 7. miR-1246 in DPSC-Exo facilitates macrophages to convert from a pro-inflammatory phenotype to an anti-inflammatory phenotype *in vitro*. (A) Relative proportion of miRNAs in the total miRNA reads. (B) miR-1246 levels in DPSC-Exo and DPSCs were analysed by RT-qPCR ($n = 6$ per group). Error bars represent SEM. $*p < 0.05$. (C) Representative density plots of phenotypic characterization of BMDMs treated with PBS, DPSC-Exo or DPSC-Exo + miR-1246 inhibitor. Gates captured single, live CD11b⁺F4/80⁺ cells. Statistical analysis of the flow cytometry data describing the MFI of CD206⁺ cells ($n = 3$). Error bars represent SEM. $*p < 0.05$. (D) Representative density plots of phenotypic characterization of BMDMs treated with PBS, DPSC-Exo or DPSC-Exo + miR-1246 inhibitor. Statistical analysis of the flow cytometry data describing the MFI of CD86⁺ cells ($n = 3$). Error bars represent SEM. $*p < 0.05$. (E) Representative density plots of phenotypic characterization of BMDMs treated with PBS or miR-1246 mimics. Gates captured single, live CD11b⁺F4/80⁺ cells. Statistical analysis of the flow cytometry data describing the MFI of CD206⁺ cells ($n = 3$). Error bars represent SEM. $*p < 0.05$. (F) Representative density plots of phenotypic characterization of BMDMs treated with PBS or miR-1246 mimics. Statistical analysis of the flow cytometry data describing the MFI of CD86⁺ cells ($n = 3$). Error bars represent SEM. $*p < 0.05$.

recent study reported that umbilical cord-derived MSCs are a new cell source for treating periodontitis [57]. However, further studies are needed to compare the therapeutic effects of exosomes from the above stem cell sources in treating periodontitis.

In this study, we expanded DPSCs in medium supplemented with FBS. However, FBS as a cell culture supplement could increase the risk of transmitting infectious bovine agents and cause xenogeneic immune reactions in patients treated with FBS-cultured stem cells or exosomes [58]. Recent studies indicate that platelet lysate (PL) is a better choice than FBS to culture stem cells for clinical use [58,59]. Therefore, exosomes derived from PL-cultured DPSCs could be a good choice for treating periodontitis in patients, but further investigations are still needed before their clinical application. DPSC-Exo are heterologous populations of extracellular vesicles (EVs) [42]. As isolation and identification of subpopulations of EVs remain a challenge [42], ongoing technological advances will help reveal their heterogeneity and biological functions and enhance their therapeutic effects in treating periodontitis. Notably, different isolation techniques can impact the purity, yield and even biological activity of exosomes [60]. UC and size exclusion chromatography (SEC) are two commonly used techniques for isolation of exosomes. Kaloyan et al. reported that UC isolates plasma exosomes of better purity but lower yield compared to those isolated by SEC [60]. Hence, different isolation methods may impact functional experiments of exosomes. In addition, UC does not sediment all

bioactive factors of DPSCs. Other bioactive factors of DPSCs that benefit the treatment periodontitis require further study.

5. Conclusions

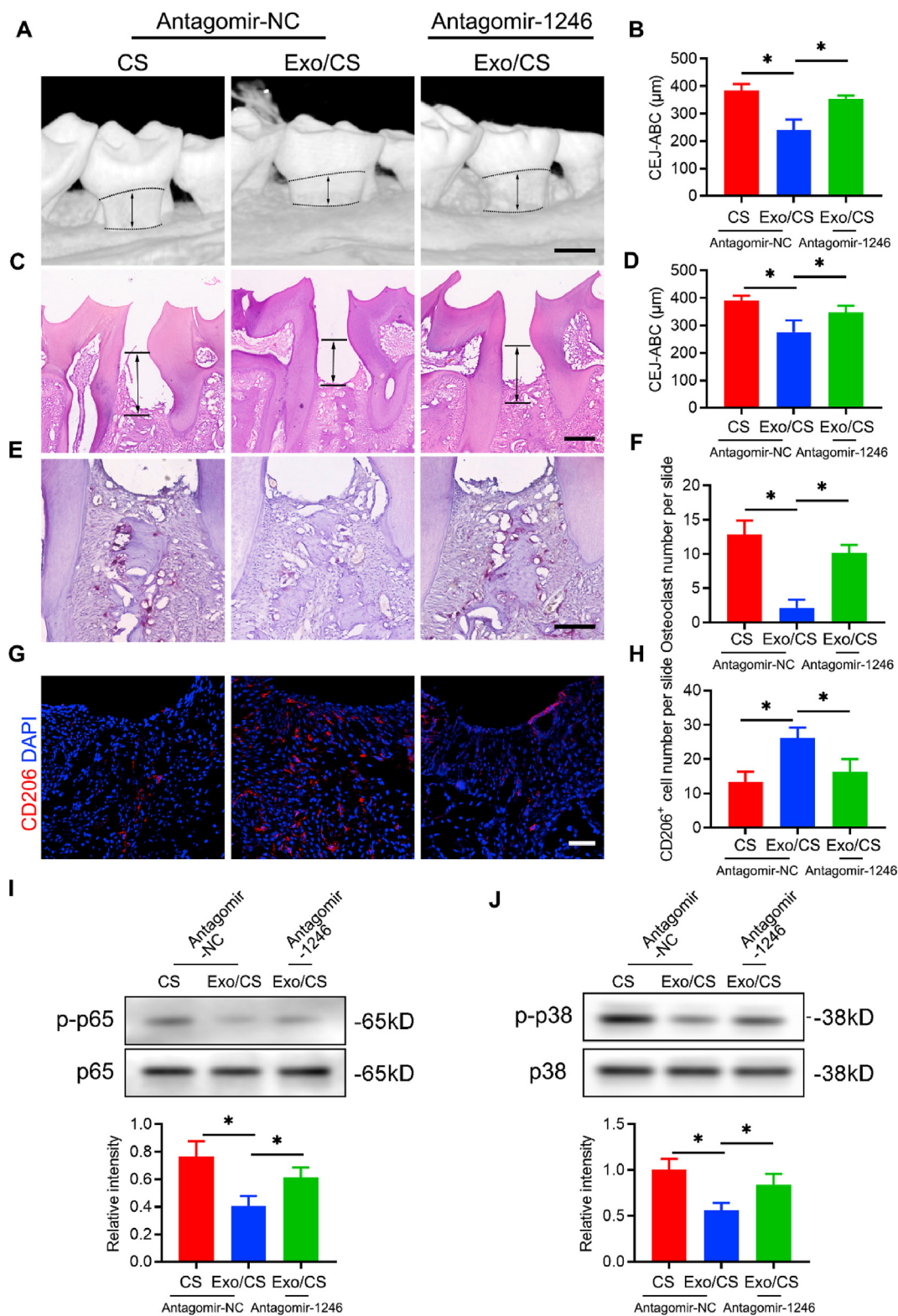
This study demonstrated that DPSC-Exo/CS can accelerate the healing of alveolar bone and the periodontal epithelium in mice with periodontitis. Remarkably, DPSC-Exo suppressed periodontal inflammation by facilitating macrophages to convert from a pro-inflammatory phenotype to an anti-inflammatory phenotype in the periodontium of mice with periodontitis. By modulating macrophage phenotype, this study provides a promising therapy for treating periodontitis.

Data availability

All experimental data to support the findings from this study will be made available to interested investigators.

CRediT authorship contribution statement

Zongshan Shen: Writing - original draft, Methodology, Conceptualization. **Shuhong Kuang:** Writing - original draft, Methodology, Software. **Yong Zhang:** Formal analysis, Validation,



(caption on next page)

Software. **Mingmei Yang:** Validation, Visualization. **Wei Qin:** Resources, Data curation. **Xuetao Shi:** Writing - review & editing, Conceptualization, Funding acquisition. **Zhengmei Lin:** Supervision, Writing - review & editing, Funding acquisition.

Declaration of competing interest

The authors declare that they have no known competing financial interests or personal relationships that could have appeared to influence the work reported in this paper.

Fig. 8. Antagomir-1246 reverses the effects of DPSC-Exo/CS in mitigating epithelial lesion and alveolar bone loss in P mice. (A) 3D reconstructions of maxillae from the PBS-, DPSC-Exo/CS- and DPSC-Exo/CS + antagomir 1246-treated groups ($n = 6$ per group) were generated by micro-CT. The vertical line extends from the CEJ to the ABC. The CEJ-ABC distance was measured at six predetermined sites on both the buccal and palatal sides. Scale bar = 400 μm . (B) Statistical analysis of the CEJ-ABC distance in each group ($n = 6$ per group) as determined by micro-CT. Error bar represents SEM. $*p < 0.05$. (C) Histological H&E-stained sections of the periodontium from each group are shown. The vertical line extends from the CEJ to the ABC. The CEJ-ABC distance was quantified in each microscope field of view. Scale bar = 200 μm . (D) Statistical analysis of the CEJ-ABC distance in each group ($n = 6$ per group) as determined by H&E staining. Error bar represents SEM. $*p < 0.05$. (E) Histological TRAP-stained sections of the periodontium from each group are shown. Osteoclasts are stained red. The number of osteoclasts was quantified in each microscope field of view. Scale bar = 100 μm . (F) Statistical analysis of the number of osteoclasts in each group ($n = 6$ per group) as determined by TRAP staining. Error bar represents SEM. $*p < 0.05$. (G) Representative IF images of CD206⁺ cells in the periodontium of each group ($n = 6$ per group). Nuclei were stained with DAPI. Scale bar = 100 μm . (H) Statistical analysis of the IF staining of periodontal CD206⁺ cells in each group ($n = 6$ per group). The number of CD206⁺ cells was quantified for each microscope field of view. Error bars represent SEM. $*p < 0.05$. (I) Representative western blots showing the NF- κB p65 signal pathway in the periodontium of each group. Statistical analysis of western blots to determine the relative intensity of NF- κB p65 signal pathway of each group ($n = 6$ per group). Error bar represents SEM. $*p < 0.05$. (J) Representative western blots showing the p38 MAPK signal pathway in the periodontium of each group. Statistical analysis of western blots to determine the relative intensity of p38 MAPK signal pathway of each group ($n = 6$ per group). Error bar represents SEM. $*p < 0.05$.

Acknowledgements

This work was supported by grants from the National Natural Science Foundation of China (Grant Nos. 81873713, 81670984 and 81700959), Science and Technology Program of Guangdong Province (2017B090911008, 2016A030306018), and the International Cooperation Project of Science and Technology in Guangdong Province (Grant No. 2016B050502008). We thank Ms. Yuwen Du from Zhongshan School of Medicine for her linguistic advice in revising the paper.

Appendix A. Supplementary data

Supplementary data to this article can be found online at <https://doi.org/10.1016/j.bioactmat.2020.07.002>.

References

- M. Sanz, A. Ceriello, M. Buyschaert, I. Chapple, R.T. Demmer, F. Graziani, D. Herrera, S. Jepsen, L. Lione, P. Madianos, M. Mathur, E. Montanya, L. Shapira, M. Tonetti, D. Vegh, Scientific evidence on the links between periodontal diseases and diabetes: consensus report and guidelines of the joint workshop on periodontal diseases and diabetes by the International Diabetes Federation and the European Federation of Periodontology, *J. Clin. Periodontol.* 45 (2) (2018) 138–149.
- D.F. Kinane, P.G. Stathopoulou, P.N. Papapanou, Periodontal diseases, *Nat Rev Dis Primers* 3 (2017) 17038.
- R. Ide, T. Hoshuyama, D. Wilson, K. Takahashi, T. Higashi, Periodontal disease and incident diabetes: a seven-year study, *J. Dent. Res.* 90 (1) (2011) 41–46.
- R. Stewart, M. West, Increasing evidence for an association between periodontitis and cardiovascular disease, *Circulation* 133 (6) (2016) 549–551.
- S.S. Dominy, C. Lynch, F. Ermini, M. Benedyk, A. Marczyk, A. Konradi, M. Nguyen, U. Haditsch, D. Raha, C. Griffin, L.J. Holsinger, S. Arastu-Kapur, S. Kaba, A. Lee, M.I. Ryder, B. Potempa, P. Mydel, A. Hellvard, K. Adamowicz, H. Hasturk, G.D. Walker, E.C. Reynolds, R.L.M. Faull, M.A. Curtis, M. Dragnow, J. Potempa, Porphyromonas gingivalis in Alzheimer's disease brains: evidence for disease causation and treatment with small-molecule inhibitors, *Science advances* 5 (1) (2019) eaau3333.
- M. Rajendran, S. Looney, N. Singh, M. Elashiry, M.M. Meghil, A.R. El-Awady, O. Tawfik, C. Susin, R.M. Arce, C.W. Cutler, Systemic antibiotic therapy reduces circulating inflammatory dendritic cells and Treg-Th17 plasticity in periodontitis, *J. Immunology* (Baltimore, Md 202 (9) (1950) 2690–2699 2019.
- C. Manresa, E.C. Sanz-Miralles, J. Twigg, M. Bravo, Supportive periodontal therapy (SPT) for maintaining the dentition in adults treated for periodontitis, *Cochrane Database Syst. Rev.* 1 (2018) CD009376.
- H.R. Preus, P. Gjerme, V. Baelum, A randomized double-masked clinical trial comparing four periodontitis treatment strategies: 5-year tooth loss results, *J. Periodontol.* 88 (2) (2017) 144–152.
- V.M. Varela, D. Heller, M.X. Silva-Senem, M.C. Torres, A.P. Colombo, E.J. Feres-Filho, Systemic antimicrobials adjunctive to a repeated mechanical and antiseptic therapy for aggressive periodontitis: a 6-month randomized controlled trial, *J. Periodontol.* 82 (8) (2011) 1121–1130.
- G. Hajishengallis, Immunomicrobial pathogenesis of periodontitis: keystones, pathogens, and host response, *Trends Immunol.* 35 (1) (2014) 3–11.
- A.J. Delima, T. Oates, R. Assuma, Z. Schwartz, D. Cochran, S. Amar, D.T. Graves, Soluble antagonists to interleukin-1 (IL-1) and tumor necrosis factor (TNF) inhibits loss of tissue attachment in experimental periodontitis, *J. Clin. Periodontol.* 28 (3) (2001) 233–240.
- M.B. Grauballe, J.A. Ostergaard, S. Schou, A. Flyvbjerg, P. Holmstrup, Effects of TNF- α blocking on experimental periodontitis and type 2 diabetes in obese diabetic Zucker rats, *J. Clin. Periodontol.* 42 (9) (2015) 807–816.
- A.J. Glowacki, S. Yoshizawa, S. Jhunjunwala, A.E. Vieira, G.P. Garlet, C. Sfeir, S.R. Little, Prevention of inflammation-mediated bone loss in murine and canine periodontal disease via recruitment of regulatory lymphocytes, *Proc. Natl. Acad. Sci. U.S.A.* 110 (46) (2013) 18525–18530.
- N. Dutzan, T. Kajikawa, L. Abusleme, T. Greenwell-Wild, C.E. Zuazo, T. Ikeuchi, L. Brenchley, T. Abe, C. Hurabielle, D. Martin, R.J. Morell, A.F. Freeman, V. Lazarevic, G. Trinchieri, P.I. Diaz, S.M. Holland, Y. Belkaid, G. Hajishengallis, N.M. Moutsopoulos, A dysbiotic microbiome triggers TH17 cells to mediate oral mucosal immunopathology in mice and humans, *Sci. Transl. Med.* 10 (463) (2018).
- K.L. Spiller, T.J. Koh, Macrophage-based therapeutic strategies in regenerative medicine, *Adv. Drug Deliv. Rev.* 122 (2017) 74–83.
- C. Garaioco-Pazmino, T. Fretwurst, C.H. Squarize, T. Berglund, W.V. Giannobile, L. Larsson, R.M. Castilho, Characterization of macrophage polarization in periodontal disease, *J. Clin. Periodontol.* 46 (8) (2019) 830–839.
- T.A. Wynn, K.M. Vannella, Macrophages in tissue repair, regeneration, and fibrosis, *Immunity* 44 (3) (2016) 450–462.
- R.P. Darveau, Periodontitis: a polymicrobial disruption of host homeostasis, *Nat. Rev. Microbiol.* 8 (7) (2010) 481–490.
- S.A. Hienz, S. Paliwal, S. Ivanovski, Mechanisms of bone resorption in periodontitis, *J. Immunol Res* 2015 (2015) 615486.
- A. Shapouri-Moghaddam, S. Mohammadian, H. Vazini, M. Taghadosi, S.-A. Esmaeili, F. Mardani, B. Seifi, A. Mohammadi, J.T. Afshari, A. Sahebkar, Macrophage plasticity, polarization, and function in health and disease, *J. Cell. Physiol.* 233 (9) (2018) 6425–6440.
- M.-Z. Zhang, B. Yao, S. Yang, L. Jiang, S. Wang, X. Fan, H. Yin, K. Wong, T. Miyazawa, J. Chen, I. Chang, A. Singh, R.C. Harris, CSF-1 signaling mediates recovery from acute kidney injury, *J. Clin. Invest.* 122 (12) (2012) 4519–4532.
- Z. Zhuang, S. Yoshizawa-Smith, A. Glowacki, K. Maltos, C. Pacheco, M. Shehabeldin, M. Mulkeen, N. Myers, R. Chong, K. Verdelis, G.P. Garlet, S. Little, C. Sfeir, Induction of M2 macrophages prevents bone loss in murine periodontitis models, *J. Dent. Res.* 98 (2) (2019) 200–208.
- O.A. Gonzalez, M.J. Novak, S. Kirakodu, A. Stromberg, R. Nagarajan, C.B. Huang, K.C. Chen, L. Orraca, J. Martinez-Gonzalez, J.L. Ebersole, Differential gene expression profiles reflecting macrophage polarization in aging and periodontitis gingival tissues, *Immunol. Invest.* 44 (7) (2015) 643–664.
- J. Galipeau, L. Sensebe, Mesenchymal stromal cells: clinical challenges and therapeutic opportunities, *Cell Stem Cell* 22 (6) (2018) 824–833.
- J. Liu, F. Yu, Y. Sun, B. Jiang, W. Zhang, J. Yang, G.T. Xu, A. Liang, S. Liu, Concise reviews: characteristics and potential applications of human dental tissue-derived mesenchymal stem cells, *Stem Cell.* 33 (3) (2015) 627–638.
- S. Lee, Q.Z. Zhang, B. Karabucak, A.D. Le, DPSCs from inflamed pulp modulate macrophage function via the TNF- α /IDO Axis, *J. Dent. Res.* 95 (11) (2016) 1274–1281.
- M. Omi, M. Hata, N. Nakamura, M. Miyabe, Y. Kobayashi, H. Kamiya, J. Nakamura, S. Ozawa, Y. Tanaka, J. Takebe, T. Matsubara, K. Naruse, Transplantation of dental pulp stem cells suppressed inflammation in sciatic nerves by promoting macrophage polarization towards anti-inflammation phenotypes and ameliorated diabetic polyneuropathy, *J. Diabetes Investigation* 7 (4) (2016) 485–496.
- C. Tran, M.S. Damaser, Stem cells as drug delivery methods: application of stem cell secretome for regeneration, *Adv. Drug Deliv. Rev.* 82–83 (2015) 1–11.
- M. Riazifar, M.R. Mohammadi, E.J. Pone, A. Yeri, C. Lasser, A.I. Segaliny, L.L. McIntyre, G.V. Shelke, E. Hutchins, A. Hamamoto, E.N. Calle, R. Crescitelli, W. Liao, V. Pham, Y. Yin, J. Jayaraman, J.R.T. Lakey, C.M. Walsh, K. Van Keuren-Jensen, J. Lotvall, W. Zhao, Stem cell-derived exosomes as nanotherapeutics for autoimmune and neurodegenerative disorders, *ACS Nano* 13 (6) (2019) 6670–6688.
- Y. Sun, H. Shi, S. Yin, C. Ji, X. Zhang, B. Zhang, P. Wu, Y. Shi, F. Mao, Y. Yan, W. Xu, H. Qian, Human mesenchymal stem cell derived exosomes alleviate type 2 diabetes mellitus by reversing peripheral insulin resistance and relieving beta-cell destruction, *ACS Nano* 12 (8) (2018) 7613–7628.
- M.C.G. Pella, M.K. Lima-Tenorio, E.T. Tenorio-Neto, M.R. Guilherme, E.C. Muniz, A.F. Rubira, Chitosan-based hydrogels: from preparation to biomedical applications, *Carbohydr. Polym.* 196 (2018) 233–245.
- K. Zhang, X. Zhao, X. Chen, Y. Wei, W. Du, Y. Wang, L. Liu, W. Zhao, Z. Han, D. Kong, Q. Zhao, Z. Guo, Z. Han, N. Liu, F. Ma, Z. Li, Enhanced therapeutic effects of mesenchymal stem cell-derived exosomes with an injectable hydrogel for

- hindlimb ischemia treatment, *ACS Appl. Mater. Interfaces* 10 (36) (2018) 30081–30091.
- [33] A. Aguilar, N. Zein, E. Harmouch, B. Hafdi, F. Bornert, D. Offner, F. Clauss, F. Fioretti, O. Huck, N. Benkirane-Jessel, G. Hua, Application of chitosan in bone and dental engineering, *Molecules* 24 (16) (2019).
- [34] X. Xu, Z. Gu, X. Chen, C. Shi, C. Liu, M. Liu, L. Wang, M. Sun, K. Zhang, Q. Liu, Y. Shen, C. Lin, B. Yang, H. Sun, An injectable and thermosensitive hydrogel: promoting periodontal regeneration by controlled-release of aspirin and erythropoietin, *Acta Biomater.* 86 (2019) 235–246.
- [35] X. Gao, Z. Shen, M. Guan, Q. Huang, L. Chen, W. Qin, X. Ge, H. Chen, Y. Xiao, Z. Lin, Immunomodulatory role of stem cells from human exfoliated deciduous teeth on periodontal regeneration, *Tissue Eng.* 24 (17–18) (2018) 1341–1353.
- [36] C. Han, J. Zhou, C. Liang, B. Liu, X. Pan, Y. Zhang, Y. Wang, B. Yan, W. Xie, F. Liu, X.Y. Yu, Y. Li, Human umbilical cord mesenchymal stem cell derived exosomes encapsulated in functional peptide hydrogels promote cardiac repair, *Biomater Sci* 7 (7) (2019) 2920–2933.
- [37] J. Marchesan, M.S. Girnary, L. Jing, M.Z. Miao, S. Zhang, L. Sun, T. Morelli, M.H. Schoenfisch, N. Inohara, S. Offenbacher, Y. Jiao, An experimental murine model to study periodontitis, *Nat. Protoc.* 13 (10) (2018) 2247–2267.
- [38] M. Tsukasaki, N. Komatsu, K. Nagashima, T. Nitta, W. Pluemsakunthai, C. Shukunami, Y. Iwakura, T. Nakashima, K. Okamoto, H. Takayanagi, Host defense against oral microbiota by bone-damaging T cells, *Nat. Commun.* 9 (1) (2018) 701.
- [39] G. Mizraji, H. Segev, A. Wilensky, A.H. Hovav, Isolation, processing and analysis of murine gingival cells, *JoVE* 77 (2013) e50388.
- [40] S. Kurgan, A. Kantarci, Molecular basis for immunohistochemical and inflammatory changes during progression of gingivitis to periodontitis, *Periodontol.* 2000 76 (1) (2018) 51–67.
- [41] C. Lo Sicco, D. Reverberi, C. Balbi, V. Ulivi, E. Principi, L. Pascucci, P. Becherini, M.C. Bosco, L. Varesio, C. Franzin, M. Pozzobon, R. Cancedda, R. Tasso, Mesenchymal stem cell-derived extracellular vesicles as mediators of anti-inflammatory effects: endorsement of macrophage polarization, *Stem Cells Transl Med* 6 (3) (2017) 1018–1028.
- [42] R. Kalluri, V.S. LeBleu, The biology function and biomedical applications of exosomes, *Science (New York, N.Y.)* 367 (6478) (2020).
- [43] X. Zhu, M. Badawi, S. Pomeroy, D.S. Sutaria, Z. Xie, A. Baek, J. Jiang, O.A. Elgamil, X. Mo, K.L. Perle, J. Chalmers, T.D. Schmittgen, M.A. Phelps, Comprehensive toxicity and immunogenicity studies reveal minimal effects in mice following sustained dosing of extracellular vesicles derived from HEK293T cells, *J. Extracell. Vesicles* 6 (1) (2017) 1324730.
- [44] A.K. Riau, H.S. Ong, G.H.F. Yam, J.S. Mehta, Sustained delivery system for stem cell-derived exosomes, *Front. Pharmacol.* 10 (2019) 1368.
- [45] J.R.J. Chew, S.J. Chuah, K.Y.W. Teo, S. Zhang, R.C. Lai, J.H. Fu, L.P. Lim, S.K. Lim, W.S. Toh, Mesenchymal stem cell exosomes enhance periodontal ligament cell functions and promote periodontal regeneration, *Acta Biomater.* 89 (2019) 252–264.
- [46] J. Huang, X. Cai, Y. Ou, L. Fan, Y. Zhou, Y. Wang, Protective roles of FICZ and aryl hydrocarbon receptor axis on alveolar bone loss and inflammation in experimental periodontitis, *J. Clin. Periodontol.* 46 (9) (2019) 882–893.
- [47] I. Kourtzelis, X. Li, I. Mitroulis, D. Grosser, T. Kajikawa, B. Wang, M. Grzybek, J. von Renesse, A. Czogalla, M. Troullinaki, A. Ferreira, C. Doreth, K. Ruppova, L.S. Chen, K. Hosur, J.H. Lim, K.J. Chung, S. Grossklaus, A.K. Tausche, L.A.B. Joosten, N.M. Moutsopoulos, B. Wielockx, A. Castrillo, J.M. Korostoff, U. Coskun, G. Hajishengallis, T. Chavakis, DEL-1 promotes macrophage efferocytosis and clearance of inflammation, *Nat. Immunol.* 20 (1) (2019) 40–49.
- [48] S. Watanabe, M. Alexander, A.V. Misharin, G.R.S. Budinger, The role of macrophages in the resolution of inflammation, *J. Clin. Invest.* 129 (7) (2019) 2619–2628.
- [49] C. Sima, A. Vinięra, M. Glogauer, Macrophage immunomodulation in chronic osteolytic diseases—the case of periodontitis, *J. Leukoc. Biol.* 105 (3) (2019) 473–487.
- [50] S. Pacios, W. Xiao, M. Mattos, J. Lim, R.S. Tarapore, S. Alsadun, B. Yu, C.Y. Wang, D.T. Graves, Osteoblast lineage cells play an essential role in periodontal bone loss through activation of nuclear factor-kappa B, *Sci. Rep.* 5 (2015) 16694.
- [51] T.E. Van Dyke, C. Sima, Understanding resolution of inflammation in periodontal diseases: is chronic inflammatory periodontitis a failure to resolve? *Periodontol.* 2000 82 (1) (2020) 205–213.
- [52] J. Wu, L. Kuang, C. Chen, J. Yang, W.N. Zeng, T. Li, H. Chen, S. Huang, Z. Fu, J. Li, R. Liu, Z. Ni, L. Chen, L. Yang, miR-100-5p-abundant exosomes derived from infrapatellar fat pad MSCs protect articular cartilage and ameliorate gait abnormalities via inhibition of mTOR in osteoarthritis, *Biomaterials* 206 (2019) 87–100.
- [53] H. Liu, Z. Liang, F. Wang, C. Zhou, X. Zheng, T. Hu, X. He, X. Wu, P. Lan, Exosomes from mesenchymal stromal cells reduce murine colonic inflammation via a macrophage-dependent mechanism, *JCI Insight* 4 (24) (2019).
- [54] J. Zhao, X. Li, J. Hu, F. Chen, S. Qiao, X. Sun, L. Gao, J. Xie, B. Xu, Mesenchymal stromal cell-derived exosomes attenuate myocardial ischaemia-reperfusion injury through miR-182-regulated macrophage polarization, *Cardiovasc. Res.* 115 (7) (2019) 1205–1216.
- [55] B. Hernandez-Monjaraz, E. Santiago-Osorio, A. Monroy-Garcia, E. Ledesma-Martinez, V.M. Mendoza-Nunez, Mesenchymal stem cells of dental origin for inducing tissue regeneration in periodontitis: a mini-review, *Int. J. Mol. Sci.* 19 (4) (2018).
- [56] Y. Zheng, C. Dong, J. Yang, Y. Jin, W. Zheng, Q. Zhou, Y. Liang, L. Bao, G. Feng, J. Ji, X. Feng, Z. Gu, Exosomal microRNA-155-5p from PDLSCs regulated Th17/Treg balance by targeting sirtuin-1 in chronic periodontitis, *J. Cell. Physiol.* 234 (11) (2019) 20662–20674.
- [57] F. Shang, S. Liu, L. Ming, R. Tian, F. Jin, Y. Ding, Y. Zhang, H. Zhang, Z. Deng, Y. Jin, Human umbilical cord MSCs as new cell sources for promoting periodontal regeneration in inflammatory periodontal defect, *Theranostics* 7 (18) (2017) 4370–4382.
- [58] J. Pierce, E. Benedetti, A. Preslar, P. Jacobson, P. Jin, D.F. Stroncek, J.A. Reems, Comparative analyses of industrial-scale human platelet lysate preparations, *Transfusion* 57 (12) (2017) 2858–2869.
- [59] G. Astori, E. Amati, F. Bambi, M. Bernardi, K. Chieregato, R. Schafer, S. Sella, F. Rodeghiero, Platelet lysate as a substitute for animal serum for the ex-vivo expansion of mesenchymal stem/stromal cells: present and future, *Stem Cell Res. Ther.* 7 (1) (2016) 93.
- [60] K. Takov, D.M. Yellon, S.M. Davidson, Comparison of small extracellular vesicles isolated from plasma by ultracentrifugation or size-exclusion chromatography: yield, purity and functional potential, *J. Extracell. Vesicles* 8 (1) (2019) 1560809.